# The Demulsification Properties of Cationic Hyperbranched Polyamidoamines for Polymer Flooding Emulsions and Microemulsions

*Authors:*

Yangang Bi, Zhi Tan, Liang Wang, Wusong Li, Congcong Liu, Zhantao Wang, Xiangchen Liu, Xinru Jia

*Abstract:*

Polymer flooding emulsions and microemulsions caused by tertiary oil recovery technologies are harmful to the environment due to their excellent stability. Two cationic hyperbranched polyamidoamines (H-PAMAM), named as H-PAMAM-HA and H-PAMAM-ETA, were obtained by changing the terminal denotation agents to H-PAMAM, which was characterized by 1H NMR, FT-IR, and amine possession, thereby confirmed the modification. Samples (300 mg/L) were added to the polymer flooding emulsion (1500 mg/L oil concentration) at 30 °C for 30 min and the H-PAMAM-HA and H-PAMAM-ETA were shown to perform at 88% and 91% deoil efficiency. Additionally, the increased settling time and the raised temperature enhanced performance. For example, an oil removal ratio of 97.7% was observed after dealing with the emulsion for 30 min at 60 °C, while 98.5% deoil efficiency was obtained after 90 min at 45 °C for the 300 mg/L H-PAMAM-ETA. To determine the differences when dealing with the emulsion, the interfacial tension, ? potential, and turbidity measurements were fully estimated. Moreover, diametrically different demulsification mechanisms were found when the samples were utilized to treat the microemulsion. The modified demulsifiers showed excellent demulsification efficiency via their obvious electroneutralization and bridge functions, while the H-PAMAM appeared to enhance the stability of the microemulsion.

# The Demulsification Properties of Cationic Hyperbranched Polyamidoamines for Polymer Flooding Emulsions and Microemulsions

**Yangang Bi** [1,2] ![ORCID], **Zhi Tan** [1,2], **Liang Wang** [1,2,*], **Wusong Li** [1,2,*], **Congcong Liu** [1,2], **Zhantao Wang** [1,2], **Xiangchen Liu** [1,2,*] and **Xinru Jia** [2,3,*]

[1] Shandong Provincial Key Laboratory of Water and Soil Conservation and Environmental Protection, Linyi University, Linyi 276000, China; longgang-54@126.com (Y.B.); cytanzhi@126.com (Z.T.); cyliucongcongsd@126.com (C.L.); cywangzhantao@126.com (Z.W.)

[2] International Dendritic and Hyperbranched Polymers Innovation and Application Center, Weihai JinHong Group Co., Ltd., Weihai 264211, China

[3] Beijing National Laboratory for Molecular Sciences, and Key Laboratory of Polymer Chemistry and Physics of the Ministry of Education, College of Chemistry and Molecular Engineering, Peking University, Beijing 100871, China

\* Correspondence: wangliang.cn@163.com (L.W.); cyliwusong@126.com (W.L.); xcliu168@126.com (X.L.); xrjia@pku.edu.cn (X.J.)

**Abstract:** Polymer flooding emulsions and microemulsions caused by tertiary oil recovery technologies are harmful to the environment due to their excellent stability. Two cationic hyperbranched polyamidoamines (H-PAMAM), named as H-PAMAM-HA and H-PAMAM-ETA, were obtained by changing the terminal denotation agents to H-PAMAM, which was characterized by $^1$H NMR, FT-IR, and amine possession, thereby confirmed the modification. Samples (300 mg/L) were added to the polymer flooding emulsion (1500 mg/L oil concentration) at 30 °C for 30 min and the H-PAMAM-HA and H-PAMAM-ETA were shown to perform at 88% and 91% deoil efficiency. Additionally, the increased settling time and the raised temperature enhanced performance. For example, an oil removal ratio of 97.7% was observed after dealing with the emulsion for 30 min at 60 °C, while 98.5% deoil efficiency was obtained after 90 min at 45 °C for the 300 mg/L H-PAMAM-ETA. To determine the differences when dealing with the emulsion, the interfacial tension, $\zeta$ potential, and turbidity measurements were fully estimated. Moreover, diametrically different demulsification mechanisms were found when the samples were utilized to treat the microemulsion. The modified demulsifiers showed excellent demulsification efficiency via their obvious electroneutralization and bridge functions, while the H-PAMAM appeared to enhance the stability of the microemulsion.

**Keywords:** cationic hyperbranched polymers; demulsifiers; polymer-flooding emulsion; microemulsion; interfacial tension; turbidity

## 1. Introduction

Surfactants that stabilize temporary emulsions play important roles in the crude oil recovery process and viscous oil transportation projects [1,2]. In particular, as a specifically desired stage in the polymer flooding oil recovery technique, partially hydrolyzed polyacryamides (PHPAMs) that can fully disperse into flooding water are frequently utilized as emulsifying agents to enhance the mobility ratio of crude oil [3,4]. However, similar typically industrial applications produce surfactant stabilized oil-in-water (O/W)-type emulsions, for example, polymer flooding emulsions and microemulsions, which can cause a series of environmental and operational issues [5,6]. It is believed that dissolved

surfactants can reduce interfacial tension by adsorbing onto the oil/water interface, thereby causing the oily waste water to possess high stabilization with firm interfacial films [7]. Although several methods exist to destabilize and separate surfactant-stabilized temporary emulsions using ternary oil recovery techniques, such as physical, biological, and chemical techniques, the problem has not yet been perfectly resolved in regard to environmental protection and energy efficiency [8–10].

One effective and applicable technique to demulsify typical O/W emulsions suggested the use of modern chemical demulsifiers, including polymer surfactants, ionic liquids, and nanoparticles [11–14]. Polymer surfactants are usually macromolecules consisting of both hydrophilic and hydrophobic portions. Such chemicals can be broadly classified into linear block polymers, natural polymeric surfactants, and dendrimers [15–17].

Traditional linear or dendritic block polymers, especially polyethers, could play a role in demulsifying O/W-type emulsions. It was reported that a slightly hydrophilic value in the hydrophilic–lipophilic balance ((HLB) = 8~10) was observed when the various ratios of ethylene oxide (EO) and propylene oxide (PO) were adjusted, which could bridge and aggregate oil droplets. However, these require higher levels of energy to destroy the stability of the emulsion [18]. Natural polymeric surfactants were recently promoted and widely researched, with advantages including their low price, widespread procurability, biodegradability, and nontoxicity. Frequently, these compounds exhibited excellent demulsification properties in regard to O/W emulsions due to their appropriate functional groups and branched-chain architectures [19–21].

Dendrimers are well-defined monodisperse macromolecules with precise structures, including original central cores, interior branches, and adjustable peripheral functional groups. They are widely used as nanocontainers for drug delivery, catalysis, and demulsifiers, as described in the research and application reports [22–24]. In particular, a higher generation of commercialized polyamidoamine (PAMAM) (G > 2.0) dendrimers were reported to exhibit fast and efficient demulsification properties benefiting from their terminal amine groups and molecular weights. Moreover, taking advantage of their empty interiors, PAMAM molecules can act as nanocontainers to attract and dissolve adsorbents left on the oil–water interface [25–27]; otherwise, they must undergo a lengthy and costly synthesis process [28–30]. As another subclass of dendritic polymers, hyperbranched PAMAMs could potentially be applicable demulsifiers due to their similar structures to perfect dendrimers in terms of their interior branches and peripheral functional groups [31,32]. Although it was believed that quaternary ammonium salts or ionic liquids performed more efficient demulsification for different kinds of emulsions [5], until now, few studies focused on cationic hyperbranched polyamidoamines as demulsifiers for polymer flooding emulsions, especially for microemulsions.

In this work, we synthesized a kind of hyperbranched polymer (H-PAMAM) using diethylenetri-amine (DETA) and methyl acrylate as the initial agents to modify its terminal amine groups into quaternary ammonium moieties by changing the modification agents in Schemes 1 and 2. The demulsification applications were estimated according to determined conditions, including the demulsifier dosage, the settling temperature, time, and the type of emulsion. It was clearly shown that quaternary ammonium moieties greatly enhanced demulsification behavior when compared with unmodified H-PAMAM under the same conditions, especially when demulsifying microemulsions. Furthermore, the structure of the cationic polymer affected the demulsification appearance, both in regard to the polymer flooding emulsion and the microemulsion using the two cationic demulsifiers, because the H-PAMAM-ETA with the more hydrophilic methyl group showed a better performance than the H-PAMAM-HA with the ethyl group. To gain insight into the demulsification mechanisms for the polymer flooding emulsion, the surface/interfacial tension, the $\zeta$ potential, and the turbidity were intrinsically analyzed [33,34]. The modified cationic polymers exhibited excellent demulsification efficiency due to the electroneutralization, while the H-PAMAM appeared as a nanocontainer to break the stability of the polymer flooding emulsion by encasing the surfactants located at the interfacial films. When treating the microemulsion, the pH affected the demulsification performance. The H-PAMAM made the microemulsion more stable than the original microemulsion due to the abundance of -NH$_2$

groups causing an alkaline pH, while the cationic hyperpolymers exhibited better demulsification performance due to their approximately neutral pH. Moreover, stronger acidic solutions and more H-PAMAM-ETA increased the demulsification efficiency.
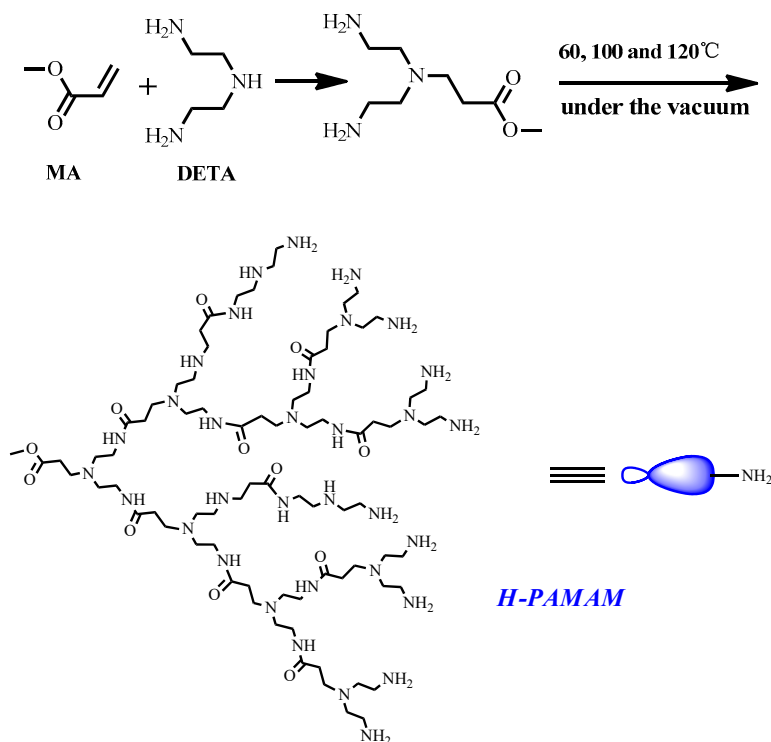


**Scheme 1.** The synthetic procedure for the demulsifier hyperbranched polyamidoamines (H-PAMAM).
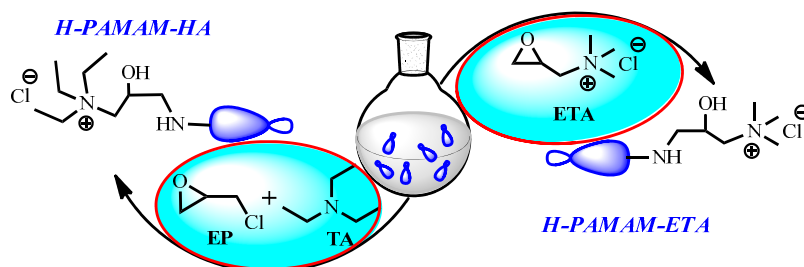


**Scheme 2.** The synthetic method for H-PAMAM-HA and H-PAMAM-ETA.

## 2. Materials and Methods

### 2.1. Chemicals

Diethylenetriamine (DETA) (99%), methyl acrylate (MA) (98.5%), methanol (99.5%), sodium lauryl sulfonate (SLS), epichlorohydrin (EP), triethylamine (TA), 1,3-epoxypropyl trimethyl- ammonium chloride (ETA), and other chemicals were commercially purchased and used without any further purification. Dehydrated crude oil was obtained from the Shengli Oilfield (Qingdao, China) and dried at 80 °C for 4 h to obtain a water content of less than 0.4% before preparing the polymer flooding O/W-type emulsions (Table S1). The microemulsion was supplied from an offshore oil field without any further treatment. Partially hydrolyzed polyacryamide (PHPAM) were obtained according to the literature [29].

## 2.2. Synthesis of the Demulsifiers

The reaction procedure for the demulsifier H-PAMAM and its modified quaternary ammonium salts are illustrated in Schemes 1 and 2, respectively. The H-PAMAM demulsifier with the DETA as the initiator were economically synthesized according to a slightly modified "one-pot" method [35]. The H-PAMAM-HA and H-PAMAM-ETA were obtained using different terminal denotation agents, as shown in Scheme 2 in the Supplementary Material.

## 2.3. Characterization of the Demulsifiers

The molecular structures of the obtained demulsifiers were recorded using $^1$H NMR characterization performed on a 400 MHz (Bruker ARX400, Billerica, MA, USA) spectrometer with $D_2O$ as the solvent at room temperature. The Fourier transform infrared (FT-IR) spectra were analyzed using a Thermo Fisher Nicolet 50 FT-IR spectrometer (Thermo Fisher, Waltham, MA, USA) with samples that were prepared as KBr pellets. The amine values were determined according to the acid–base titration method.

## 2.4. Preparation of Oil-in-Water Emulsions

### 2.4.1. The Polymer Flooding Emulsion

Crude oil ($\eta$50 °C = 353.7 mPa·s, $\rho$25 °C = 0.97 g/cm$^3$, 5.0 g, Table S1), PHPAM (0.3 g), and sodium lauryl sulfonate (SLS) (0.3 g), were successively added into a conical flask. Then, 1000 g of deionized water was added and violently stirred using a mulser at 10,000 rpm/min for 5 min [28,30]. Ultimately, the simulated crude O/W emulsion was collected after separating the floating oil phase on the surface; 1500 mg/L of oil was recorded using a Varian CARY 1E UV-Vis spectrophotometer (Varian Medical Systems (VAR), Palo Alto, CA, USA). The pH value of the emulsion was evaluated as weakly acidic at a pH of 5. The obtained emulsion stayed stable for about 1 week without changing the room temperature.

### 2.4.2. The Microemulsion

A kind of microemulsion was obtained from one offshore oil field and used without any treatment. The emulsion was found to be stable for more than 6 months at room temperature. Moreover, its transmittance at 400 nm was only 1.04% when it was estimated by the Varian CARY 1E UV-Vis spectrophotometer.

## 2.5. Demulsification Tests

### 2.5.1. Demulsification Tests on the Polymer Flooding Emulsion

To appraise the designed demulsifiers performances, standard bottle tests were recorded using serial setting conditions. Specific proportions of the freshly prepared O/W emulsions and demulsifiers were combined in capped cylinders and shaken at least 200 times to uniformly mix the ingredients at a frequency of 2 shakes/s [30]. Later, all of the comparable bottles were placed in a series of water baths at confirmed temperatures and left to settle for certain periods of time. Thereafter, the aqueous phases were cooled to room temperature and pre-extracted and finely separated using petroleum ether after adding 1 mL hydrochloric acid to 10 mL of the emulsion. Subsequently, the residual oil contents were obtained from the petroleum ether phases, which were recorded using the UV-Vis spectrophotometer. Finally, the demulsification efficiency of the designed materials was evaluated using the following formula:

$$DR = (C_0 - C)/C_0 \times 100\% \tag{1}$$

where $DR$ (%) represents the demulsification ratio, $C_0$ (mg/L) represents the initial oil content, and $C$ (mg/L) refers to the extracted oil concentration from the water phase before and after demulsification using the petroleum ether.

2.5.2. Demulsification Tests on the Microemulsion

The microemulsion was another kind of O/W emulsion that was found during the oil recovery. It was more stable (>6 months) than the polymer flooding emulsions, and its particle size was at the nanometer level, which could not be observed under the microscope like the polymer flooding emulsion. In addition, it was found that the microemulsion could not be destroyed by adding 1 mL of hydrochloric acid to extract the oil droplets before and after demulsification, and the pH value of the microemulsion was 7. Thus, considering that the microemulsion was a transparent solution before and after demulsification, the abilities of the demulsifier were characterized using the transmittance recorded by the UV-Vis spectrophotometer at 400 nm.

## 3. Results and Discussion

### 3.1. Characterization of the Demulsifiers

The characteristic parameters for the demulsifiers, i.e., H-PAMAM, H-PAMAM-HA, and H-PAMAM-ETA, were extracted from the $^1$H NMR and FT-IR characterizations. Figure 1 and Figures S1–S3 show the representative $^1$H NMR spectra of the demulsifiers. The $^1$H NMR signals that represent the amine groups (~2.0 ppm) were not present in the H-PAMAM-HA and H-PAMAM-ETA spectra. In addition, the absorption peaks for -CH$_2$-, which ranged from 2.29 to 3.47 ppm, revealed a characteristic broad resonance of the hyperbranched groups, which slightly increased in the modified products. Moreover, obvious -CH$_3$ peaks were recorded, which belonged to the exyl groups (1.35 ppm) of H-PAMAM-HA and –N(CH$_3$)$_3$ (3.24 ppm) for H-PAMAM-ETA. Moreover, the signals observed around at 3.69 ppm presented the appearance of ester groups according to the designed structures of the demulsifiers in Schemes 1 and 2.
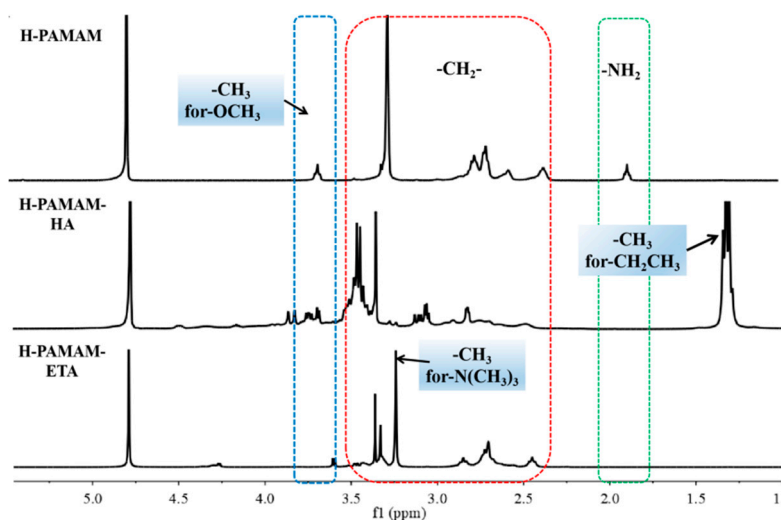


**Figure 1.** The $^1$H NMR spectra of the demulsifiers.

The FT-IR spectra of the demulsifiers are depicted in Figure S4. Bi-modal absorption peaks representing amine groups were displayed at 3414.88 cm$^{-1}$, which turned to be broad band signals of -OH and amine groups for H-PAMAM-HA and H-PAMAM-ETA. Correspondingly, stronger values for -CH$_3$ were observed at about 2948.8 cm$^{-1}$ and 964 cm$^{-1}$, which belonged to the quaternary ammonium salts.

In addition, the amine values changed from 130 mg KOH/g to 35 mg KOH/g and 40 mg KOH/g for H-PAMAM-HA and H-PAMAM-ETA, respectively, thereby proving the modification of H-PAMAM according to the 1H NMR and FT-IR spectra.

### 3.2. Effects on Demulsification on the Polymer Flooding Emulsion

The systematic investigation into the demulsification performances regarding the polymer flooding emulsion was evaluated under determined conditions, including the demulsifier concentration, the settling temperature, and the holding time.

3.2.1. Effect of Concentration

The demulsifier dosage played an important role in separating the O/W emulsions. To evaluate the performance in various dosages, the concentrations of three demulsifiers were set as 50, 100, 150, 200, 250, and 300 mg/L when added into the emulsion. After 30 min in the same water bath (at 30 °C), the oil removal rates were recorded according to the aforementioned method; these results are shown in Figure 2.
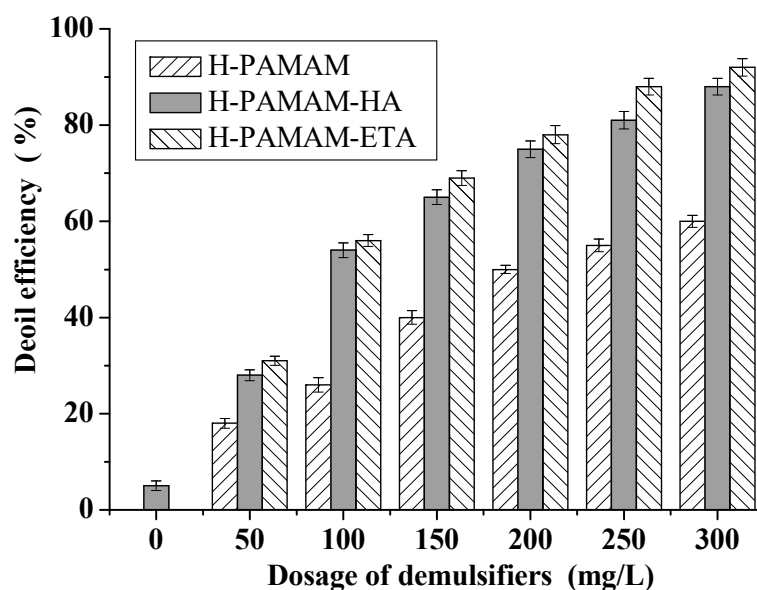


**Figure 2.** Demulsifier performance in different dosages at 30 °C for 30 min.

The blank case with no demulsifier exhibited a mere 5% oil removal ratio under the same conditions (see Table S2 and Figure S5), illustrating that the emulsion was stable enough during the demulsification. As shown in Figure S5, the concentrations of the demulsifier samples dramatically influenced their appearances. The demulsification efficiency at a 50 mg/L demulsifier dosage added to the emulsions ranged from 18% to 32%. Obviously, the more demulsifier that was added to an emulsion, the better the demulsification performance was. The oil removal rates reached 88% and 91% for H-PAMAM-HA and H-PAMAM-ETA, respectively, but only 60% for H-PAMAM at a concentration of 300 mg/L. During the emulsion separation, the synergies were closely related to the hyperbranched structures and appropriate molecular modifications of the hyperbranched demulsifiers. Thus, the positively charged branches made the demulsifier molecules dissolve more easily into the water phase, thereby allowing them to easily migrate to the oil–water interface due to the terminal alkyl groups of H-PAMAM-HA and H-PAMAM-ETA. At the same time, the negative surfactants and the demulsification molecules were electrically neutralized immediately. Finally, the oil–water interfacial film was broken up and oil droplets coalesced with each other. The H-PAMAM-ETA performed better than H-PAMAM-HA, potentially due to the terminal alkyl groups. The $-N(CH_3)_3$ in the H-PAMAM-ETA showed slightly better hydrophilicity and less steric hindrance than the $-N(CH_2CH_3)$ in H-PAMAM-HA, resulting in the H-PAMAM-ETA having a stronger interaction with the surfactants, such as SLS, which was proven according to the interfacial tension measurements and the turbidity results.

3.2.2. Effect of Temperature

The aforementioned demulsification temperature was set at 30 °C to simulate the low-temperature reservoir conditions. Another two representative temperatures at 45 and 60 °C were chosen as references against the medium-low and high temperature reservoirs of typical Chinese oilfields, respectively. All the experiments in this section were left to settle consistently for 30 min at three different temperatures.

As shown in Figure 3, the relationship between the oil removal ratio and temperature were investigated. The oil removal ratio varied obviously during the demulsification process due to both temperature and demulsifier dosage. In particular, the temperature significantly influenced and enhanced the demulsifier performance when less (100 mg/L) demulsifier was added to the emulsion. The H-PAMAM removed 74.8% of oil from the emulsion, while the oil removal values of H-PAMAM-HA and H-PAMAM-ETA were 82.4% and 88.3%, respectively, with a demulsifier concentration of 100 mg/L and a settling time of 30 min at 60 °C. However, the oil removal rates were 26%, 54%, and 56% at 30 °C for 30 min, respectively. Better deoil efficiency than H-PAMAM (89.3%) was exhibited by H-PAMAM-HA (95.7%) and H-PAMAM-ETA (97.7%) using 300 mg/L of the modified products as the demulsifiers added to the emulsions at 60 °C for 30 min, while a lower oil removal rate was observed at 60.2%, 88.3%, and 92.1% at 30 °C for 30 min, respectively.
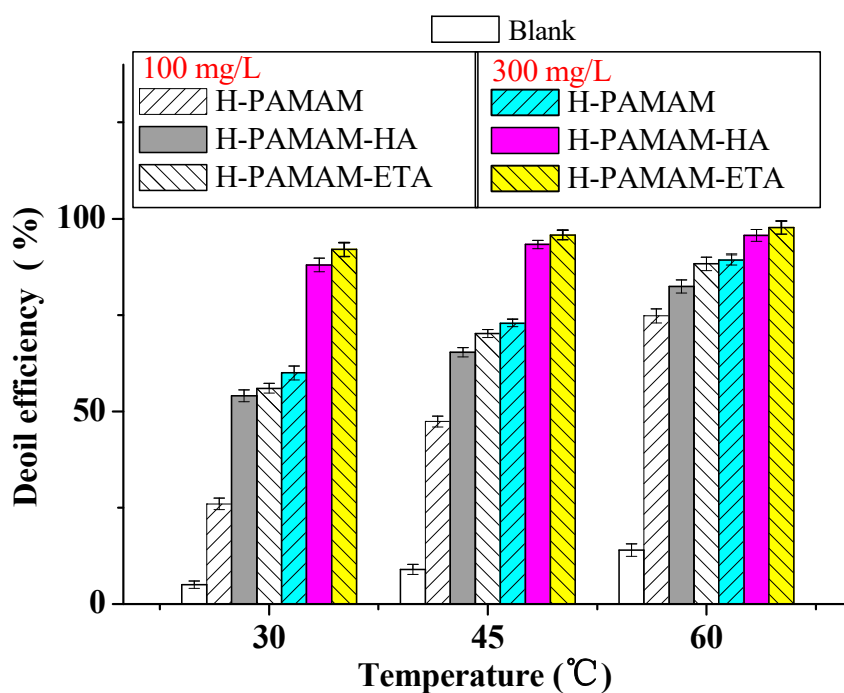


**Figure 3.** The changes in the deoil efficiency versus temperature with 100 and 300 mg/L demulsifier concentrations with settling times of 30 min, respectively.

These better performances may have been due to the variation of the temperature. On one hand, increasing the temperature of the emulsion may have made the oil droplets become less viscous and collide with each other more frequently. Thus, the molecules of the emulsion-breaking agents may more easily have reached and rapidly adhered to the oil–water interface, thereby reducing the interfacial film and promoting the discrepancy of densities between the phases. On the other hand, the neutralization between the demulsifiers and the electronegative surfactant may have increased the demulsification efficiency. Furthermore, higher temperatures caused weaker hydrogen bonding between the surfactants and the oil drops, thereby affecting their solubility in the water phase. Thus, effective surfactant concentration at the interface decreased, causing increased coalescence of the oily

droplets. It appeared that higher temperatures remarkably accelerated the emulsion-separating process and improved demulsification efficiency.

### 3.2.3. Effect of Settling Time

The settling time was another vital factor that obviously affected the demulsification accomplishment of the hyperbranched polymers. As shown in Figure 4, the bottles were left to settle for 30 min, 60 min, and 90 min, respectively. It was observed that the emulsion was stable enough during the settlement according to the reference blank experiments. Moreover, the oil removal ratio rose with the settling time when the water bath was kept at 45 °C with either 100 mg/L or 300 mg/L of demulsifier. Initially, the performance of H-PAMAM appeared to be more time-dependent than the other two modified hyperbranched demulsifiers. However, they all exhibited larger demulsification rate versus time slopes in the first treatment stage (from 30 min to 60 min) than the second, where the demulsification achieved its maximum rate and the systems gradually reached equilibrium.
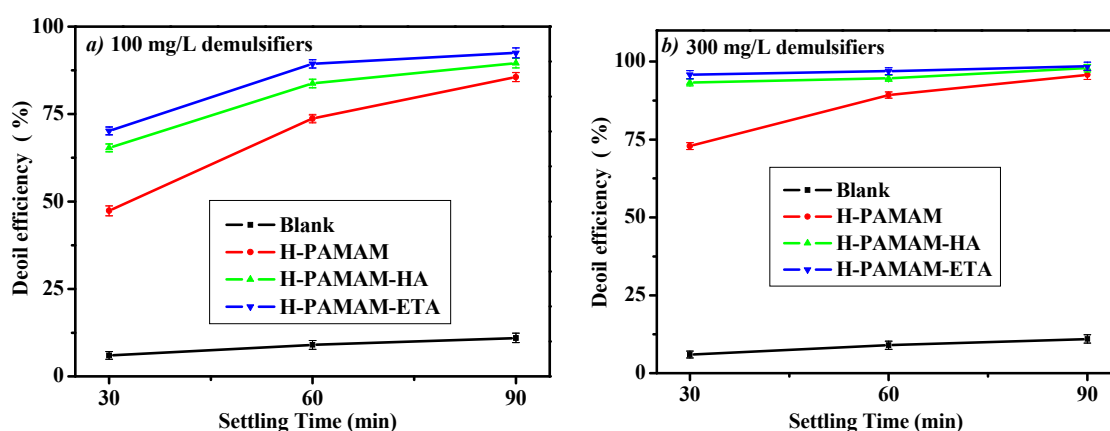


**Figure 4.** The deoil efficiency versus the settling time at 45 °C (**a**) for 100 mg/L demulsifier and (**b**) for 300 mg/L demulsifier.

Relatively, the excellent demulsification efficiency contributed to the abundance of polar terminal groups, as well as the particular hyperbranched composition. As previously mentioned, the pH value of the emulsion was 5, so the protonated amine groups and the cationic quaternary ammonium moiety aided the demulsifier molecules' electrostatic repulsion to each other. Comprehensively, together with their highly branched structures, the demulsifier molecules were more multipoint and easily stuck to the oil–water interface, thereby electroneutralizing the surfactant, altering the interfacial tensions, reducing the intensity of the interfacial film, and obtaining outstanding properties (96.9% and 98.5% oil removal ratios for 300 mg/L H-PAMAM-HA and H-PAMAM-ETA, respectively) in 90 min.

Since the emulsion was classified as both a thermodynamically and dynamically unstable system, the internal structure of the demulsifier molecules and their external factors, such as higher temperatures, greater dosages, and longer processing times, played synthetic roles in destroying the emulsion. Thus, to explore the internal deoil mechanisms of the three designed hyperbranched demulsifiers when dealing with the polymer flooding emulsion, several measurements, such as the surface/interfacial tension and ζ potential, were applied as follows.

### 3.2.4. Interfacial Activity of Demulsifiers

The static surface and interfacial tensions were measured using an interfacial tensiometer (Dataphysics DCAT21, China). The static surface tensions of the demulsifiers in the water solution were measured from 71.46 to 67.95 mN/m with dosages ranging from 0 to 600 mg/L at room temperature; these values varied slightly from the pure water due to their abundance of polar terminal groups. Initially, the interfacial tension of the oil–water interface was 28.35 mN/m, as shown in Figure 5.

This reduction indicated that the surfactant promoted the stabilization of the prepared emulsion. The oil–water interface with different dosages of demulsifiers are also illustrated in Figure 5.
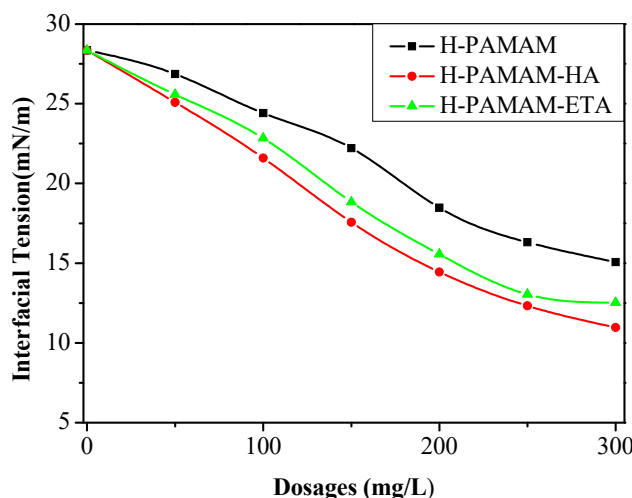


**Figure 5.** The interfacial tension versus the dosages of the demulsifiers at room temperature.

From Figure 5, H-PAMAM and its derivatives gradually reduced the interfacial tension, and the balance of interfacial tension using different dosages of demulsifiers was measured from 26.89 to 10.97 mN/m. Clearly, the results of the interfacial tension with the aforementioned demulsification performance, as shown in Figure 1, showed a positive correlation, namely, the demulsifier dosage played an important role in neutralizing the surfactants and demulsifying the polymer flooding emulsion. The modified demulsifiers exhibited lower interfacial tension than the original H-PAMAM. Thus, it was concluded that both the special hyperbranched topological structure and the terminal amine groups efficiently decreased the oil–water interfacial tension by rapidly inserting themselves into the interfacial film and partially substituting the intrinsic surfactants. In accordance with the interaction results between the demulsifiers and SLS, as seen in Figure 6, the positively charged branches of the demulsifiers spontaneously attracted more dispersed oil droplets and immediately induced electrostatic charge neutralization. Eventually, they caused emulsion destruction and oil droplet coalescence. Moreover, the H-PAMAM-ETA appeared to have the highest interfacial tension but a slightly better demulsification performance. These results indicated that the structure of the polymers affected their appearance, because the ethyl exhibited slightly more hydrophobicity and more steric hindrance than the methyl group in H-PAMAM-ETA.
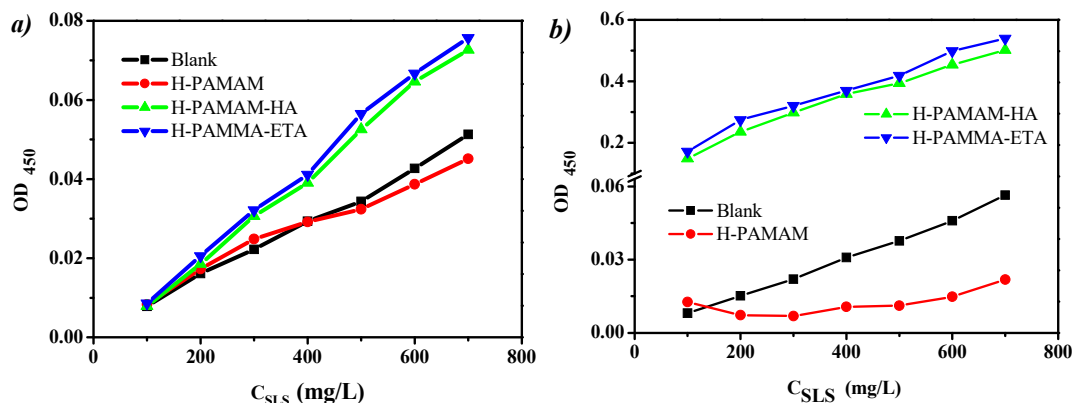


**Figure 6.** The turbidity measurements of the demulsifier–sodium lauryl sulfonate (SLS) mixtures using an optical density of 450 nm for (**a**) data obtained immediately with/without demulsifiers and (**b**) data recorded after letting the mixtures settle for 24 h.

### 3.2.5. ζ Potential

To gain further insight into demulsification process, the ζ potential measurements of the mixtures were obtained with and without adding various dosages of demulsifiers to the emulsion at 30 °C. Consequently, we found that the original ζ potential before adding the demulsifiers was negative, with an average value of −15.23 ± 0.45 mV, indicating that the stabilization of the freshly prepared emulsion could be attributed to the electrostatic repulsion among the dispersed electronegative oil droplets in addition to the reduced interfacial tension, as shown in Figure 5. Notably, after demulsifying the emulsions with 300 mg/L H-PAMAM, H-PAMAM-HA, and H-PAMAM-ETA, the ζ potentials were −0.43 ± 0.45, 0.92 ± 0.43, and 0.89 ± 0.48 mV, respectively. The variations of the ζ potentials indicated that the charged neutralization process positively promoted demulsification. Additionally, H-PAMAM-ETA exhibited slightly higher positive values than H-PAMAM-HA, showing that the arrangement and typical terminal groups of the hyperbranched polymer affected the performance when breaking up the O/W polymer flooding emulsion. Thus, the hyperbranched polymers benefited from comprehensive factors, including the framework arrangement, the terminal groups, and the spontaneous electroneutralization when the polymer flooding emulsion was demulsified.

### 3.2.6. Turbidity

As shown in Figure 6, to evaluate mutual adsorption, the metrological SLS solutions were mixed with 100 mg/L demulsifier (water–SLS–demulsifier system) and turbidity was measured using a wavelength of 450 nm optical density transmission [36]. Two different conditions were specified to clarify the interaction between the demulsifiers and the dispersed surfactants. The as-prepared solutions were immediately detected (Figure 6a) and measured 24 h later to see if equilibrium was reached (Figure 6b).

From Figure 6, the optical density transmission of the SLS solutions increased with the gradually additional concentration ($C_{SLS}$); moreover, they appeared stable due to slight observed changes 24 h later at room temperature. However, as illustrated, the as-prepared mixtures exhibited incremental turbidity when they were measured after the addition of a demulsifier under two different conditions. Obviously, the interaction forces between the demulsifier and SLS molecules were strong enough to be easily observed and evaluated by optical density when 100 mg/L demulsifier was added to the SLS solutions, as seen in Figure 6a. Initially, the optical densities showed slight changes and were approximate to the SLS solution results at a lower concentration ($C_{SLS} \leq 200$ mg/L) after adding the demulsifier. However, significant differences were observed when $C_{SLS} > 200$ mg/L, in particular when it was over 400 mg/L. The turbidity of the modified demulsifiers exhibited higher values than those observed when H-PAMAM was added and the original SLS solution. Thus, in accordance with the results in Figures 5 and 6, the quaternary ammonium salts immediately interacted with the surfactants via charge neutralization and electrostatic interactions, while the H-PAMAM mainly adsorbed and encased the SLS to achieve acceptable demulsification efficiency via hydrogen bonds and electrostatic interactions.

As shown in Figure 6b, more information would confirm the above hypothesis; the turbidity data showed the mixtures approaching equilibrium 24 h later. The divergent values between the modified and original demulsifiers showed the different demulsification mechanisms, illustrating that the H-PAMAM exhibited better transmission than the pure SLS solutions ($C_{SLS} \geq 200$ mg/L), while the modified demulsifiers demonstrated severe turbidity. In accordance with their demulsification, the additional settling time and demulsifier dosages tended to promote both charge neutralization and adsorption performance on the surfactant.

### 3.2.7. Demulsification Mechanism

Due to the measurements discussed above, a possible demulsification mechanism for H-PAMAM-HA and H-PAMAM-ETA was formulated, as shown in Figure 7. Initially, as illustrated in

Figure 7a, oil droplets that ranged from 5 to 35 μm were found to freely disperse in the O/W emulsions. As soon as a cationic demulsifier was added (Figure 7b), negative surfactants were attracted, including SLS, PHPAM, and asphaltene, which existed on the surface of the oil droplets, causing a reduction in interfacial tension and enhancing the coalescence of the oil droplets. The diameter of the oil droplets ranged between 30 and 100 μm. This phenomenon was attributed to the spontaneous neutralization between the surfactants and the demulsifiers in accordance with the ζ potential measurement. In the end, the polymer flooding emulsion separated into its water and oil phases.
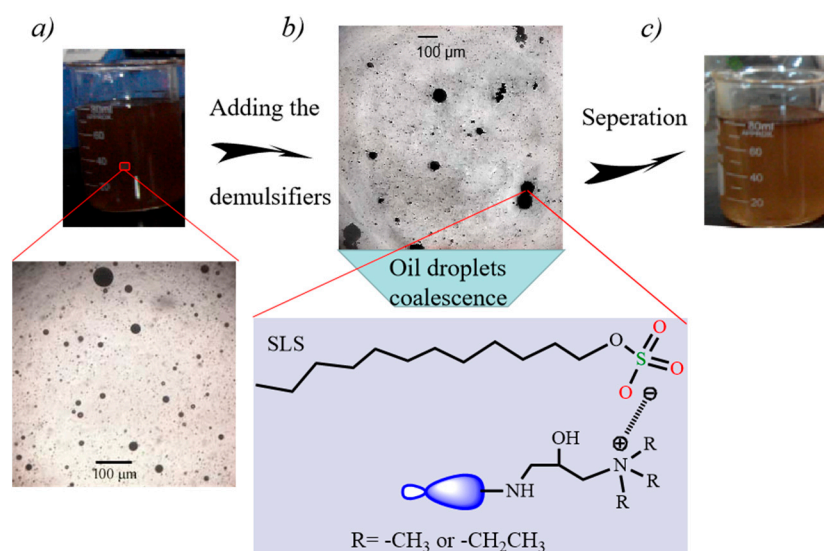


**Figure 7.** The demulsification mechanisms of H-PAMAM-HA and H-PAMAM-ETA. (**a**) The emulsion and its microstructure obtained under microscope; (**b**) oil droplet coalescence and possible neutralization between the surfactant and the demulsifier; (**c**) the separation process.

### 3.3. Effects of Demulsification on the Microemulsion

H-PAMAM and its cationic derivatives, H-PAMAM-HA and H-PAMAM-ETA, were observed to destroy the stability of the polymer flooding emulsion according to the aforementioned measurement results. The cationic demulsifiers obtained excellent demulsification efficiency, however, we tried to demulsify a more stable O/W-type emulsion, the microemulsion, using synthesized demulsifiers, and the microemulsion was shown to be quite different from the polymer flooding emulsion. For example, the oil droplets of the polymer flooding emulsion were between 5 to 35 μm, as seen in Figure 7a, while the oil droplets of the microemulsion could not be effectively observed under the same microscope. Moreover, the microemulsion appeared as a transparent yellow liquid, as seen in Figures S6 and S7.

Initially, 80 mg/L of H-PAMAM was found to make the microemulsion more stable due to the transmittance of the microemulsion changing from 1.04% to 0.74% at 60 °C for 30 min. However, 80 mg/L of H-PAMAM-HA and H-PAMAM-ETA obtained better transmittance with 7.22% and 7.66% under the same conditions, respectively. Thus, only the application of H-PAMAM-ETA was discussed under different dosages and pH values at 60 °C to verify its demulsification effect (Figure 8). The pH tended to be the crucial parameter in the use of H-PAMAM-ETA as the demulsifier to break the stability of such microemulsion.
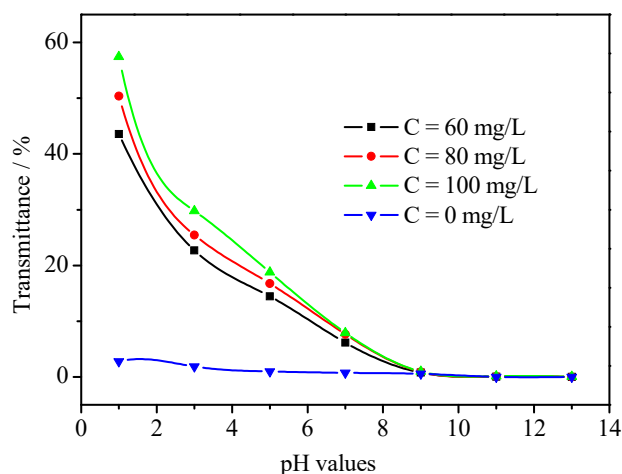
**Figure 8.** The utilization of H-PAMAM-ETA at different pH values and dosages for demulsification of the microemulsion.

As shown in both Figure 8 and Figure S6, although the transmittance after adjusting the microemulsion to different pH values showed little variation without any demulsifier, the H-PAMAM-ETA transmittance was dramatically higher in the acidic microemulsion. Indeed, the acidic pH played an important role in promoting the demulsification of H-PAMAM-ETA, and the microemulsion became more and more clear when the pH value changed from 7 to 1. This phenomenon might have been due to the branches opening as a result of the electrostatic repulsion, which allowed the demulsifier to more easily bridge the surfactants in the microemulsion. In addition, higher dosages exhibited better demulsification efficiency, due to more simultaneous adsorption of the surfactants.

## 4. Conclusions

Hyperbranched polyamidoamines (H-PAMAM) with DETA as the initiator were modified into two kinds of quaternary ammonium salts, which were both successfully synthesized as confirmed by ^{1}H NMR, FT-IR, and amine values. The modified demulsifiers displayed better performances than H-PAMAM when they were applied to demulsify both the polymer flooding O/W emulsion and the microemulsion. An oil removal ratio as high as 97.7% was observed for the modified demulsifiers that treated the polymer flooding emulsion after 30 min at 60 °C. According to the interfacial tension, $\zeta$ potential, and turbidity data, acceptable demulsification properties may have contributed to the collaborative results from the effects of both the hyperbranched structures and the modified terminal cationic groups. On the other hand, the modified polymers exhibited diametrically different demulsification efficiency levels when dealing with the microemulsion from the H-PAMAM, because the cationic moiety appeared to promote the demulsifiers to exhibit high interfacial activity, thereby destroying the stability of the typical microemulsions by adsorbing the surfactants. However, the pH values dramatically influenced the H-PAMAM-ETA performance. It is believed that bridge function between demulsifiers and surfactants can be enhanced by stretched branched chains of cationic demulsifiers due to the electrostatic repulsion under acidic conditions. Thus, the cationic modified hyperbranchend polymers investigated in this work provide a promising strategy for the demulsification of both polymer flooding emulsions and microemulsions.

**Author Contributions:** Conceptualization, Y.B., W.L., and X.J.; data curation, Y.B., Z.T., L.W., W.L., C.L., and X.L.; formal analysis, Y.B., Z.T., and Z.W.; investigation, Y.B., Z.T., W.L., and X.J.; methodology, Y.B.; project administration, X.J.; resources, W.L. and X.J.; supervision, L.W.; writing—original draft, Y.B.; writing—review and editing, L.W., W.L., X.L., and X.J. All authors read and agreed to the published version of the manuscript.

**Conflicts of Interest:** The authors declare no conflict of interest.

## References

1. Trowbridge, A.; Reich, D.; Gaunt, M.J. Multicomponent synthesis of tertiary alkylamines by photocatalytic olefin-hydroaminoalkylation. *Nature* **2018**, *561*, 522–527. [CrossRef] [PubMed]

2. Wang, Z.; Wang, Y.; Liu, G. Rapid and Efficient Separation of Oil from Oil-in-Water Emulsions Using a Janus Cotton Fabric. *Angew. Chem.* **2016**, *128*, 1313–1316. [CrossRef]

3. Zolfaghari, R.; Fakhru L-Razi, A.; Abdullah, L.C.; Elnashaie, S.S.E.H.; Pendashteh, A. Demulsification techniques of water-in-oil and oil-in-water emulsions in petroleum industry. *Sep. Purif. Technol.* **2016**, *170*, 377–407. [CrossRef]

4. Musevic, I. Two-Dimensional Nematic Colloidal Crystals Self-Assembled by Topological Defects. *Science* **2006**, *313*, 954–958. [CrossRef]

5. Shehzad, F.; Hussein, I.A.; Kamal, M.S.; Ahmad, W.; Sultan, A.S.; Nasser, M.S. Polymeric Surfactants and Emerging Alternatives used in the Demulsification of Produced Water: A Review. *Polym. Rev.* **2018**, *58*, 63–101. [CrossRef]

6. Grenoble, Z.; Trabelsi, S. Mechanisms, performance optimization and new developments in demulsification processes for oil and gas applications. *Adv. Colloid Interface Sci.* **2018**, *260*, 32–45. [CrossRef]

7. Rajak, V.K.; Singh, I.; Kumar, A.; Mandal, A. Optimization of separation of oil from oil-in-water emulsion by demulsification using different demulsifiers. *Petrol. Sci. Technol.* **2016**, *34*, 1026–1032. [CrossRef]

8. Putatunda, S.; Bhattacharya, S.; Sen, D.; Bhattacharjee, C. A review on the application of different treatment processes for emulsified oily wastewater. *Int. J. Environ. Sci. Technol.* **2019**, *16*, 2525–2536. [CrossRef]

9. Wu, J.; Zhang, J.; Kang, Y.; Wu, G.; Chen, S.C.; Wang, Y.Z. Reusable and Recyclable Superhydrophilic Electrospun Nanofibrous Membranes with In Situ Co-cross-linked Polymer-Chitin Nanowhisker Network for Robust Oil-in-Water Emulsion Separation. *ACS Sustain. Chem. Eng.* **2018**, *6*, 1753–1762. [CrossRef]

10. Atta, A.M.; Abdullah, M.M.S.; Al-Lohedan, H.A.; Ezzat, A.O. Demulsification of heavy crude oil using new nonionic cardanol surfactants. *J. Mol. Liq.* **2018**, *252*, 311–320. [CrossRef]

11. Atta, A.M.; Abdullah, M.M.S.; Al-Lohedan, H.A.; Gaffer, A.K. Synthesis and Application of Amphiphilic Poly(ionic liquid) Dendron from Cashew Nut Shell Oil as a Green Oilfield Chemical for Heavy Petroleum Crude Oil Emulsion. *Energy Fuel* **2018**, *32*, 4873–4884. [CrossRef]

12. Salehizadeh, H.; Yan, N.; Farnood, R. Recent advances in polysaccharide bio-based flocculants. *Biotechnol. Adv.* **2018**, *36*, 92–119. [CrossRef] [PubMed]

13. Kwon, G.; Panchanathan, D.; Mahmoudi, S.R.; Gondal, M.A.; McKinley, G.H.; Varanasi, K.K. Visible light guided manipulation of liquid wettability on photoresponsive surfaces. *Nat. Commun.* **2017**, *8*, 14968. [CrossRef] [PubMed]

14. Schwarz, S.; Jaeger, W.; Paulke, B.R.; Bratskaya, S.; Smolka, N.; Bohrisch, J. Cationic Flocculants Carrying Hydrophobic Functionalities: Applications for Solid/Liquid Separation. *J. Phys. Chem. B* **2007**, *111*, 8649–8654. [CrossRef]

15. Ma, J.; Fu, K.; Shi, J.; Sun, Y.; Zhang, X.; Ding, L. Ultraviolet-assisted synthesis of polyacrylamide-grafted chitosan nanoparticles and flocculation performance. *Carbohyd. Polym.* **2016**, *151*, 565–575. [CrossRef]

16. Tong, J.; Wei, Z.; Yang, H.; Yang, Z.; Chen, Y. Study on the phase transition behaviors of thermoresponsive hyperbranched polyampholytes in water. *Polymer* **2016**, *84*, 107–116. [CrossRef]

17. Liu, J.; Li, X.; Jia, W.; Li, Z.; Zhao, Y.; Ren, S. Demulsification of Crude Oil-in-Water Emulsions Driven by Graphene Oxide Nanosheets. *Energy Fuel* **2015**, *29*, 4644–4653. [CrossRef]

18. Wang, F.; Zhang, Z.; Wang, T.; Li, Y.; Cui, M. Synthesis, Characterization, and Demulsification Behavior of Amphiphilic Dendritic Block Copolymers. *J. Disper. Sci. Technol.* **2015**, *36*, 1097–1105. [CrossRef]

19. Haase, M.F.; Brujic, J. Tailoring of High-Order Multiple Emulsions by the Liquid-Liquid Phase Separation of Ternary Mixtures. *Angew. Chem. Int. Ed.* **2014**, *53*, 11793–11797. [CrossRef]

20. Abdulraheim, A.M. Green polymeric surface active agents for crude oil demulsification. *J. Mol. Liq.* **2018**, *271*, 329–341. [CrossRef]

21. Lü, T.; Zhang, S.; Qi, D.; Zhang, D.; Zhao, H. Enhanced demulsification from aqueous media by using magnetic chitosan-based flocculant. *J. Colloid Interface Sci.* **2018**, *518*, 76–83. [CrossRef] [PubMed]

22. Caminade, A.; Yanc, D.; Smith, D.K. Dendrimers and hyperbranched polymers. *Chem. Soc. Rev.* **2015**, *44*, 3870–3873. [CrossRef] [PubMed]

23. Zhang, Z.; Xu, G.; Wang, F.; Dong, S.; Chen, Y. Demulsification by amphiphilic dendrimer copolymers. *J. Colloid Interface Sci.* **2005**, *282*, 1–4. [CrossRef]

24. Ghasempour, A.; Pajootan, E.; Bahrami, H.; Arami, M. Introduction of amine terminated dendritic structure to graphene oxide using Poly propylene Imine) dendrimer to evaluate its organic contaminant removal. *J. Taiwan Inst. Chem. E* **2017**, *71*, 285–297. [CrossRef]

25. Wang, J.; Li, C.Q.; Qu, H.J.; Hu, F.L.; Yang, Y. Terminal Group Effects on Demulsification Using Dendrimers. *Petrol. Sci. Technol.* **2010**, *28*, 883–891. [CrossRef]

26. Yao, X.; Jiang, B.; Zhang, L.; Sun, Y.; Xiao, X.; Zhang, Z.; Zhao, Z. Synthesis of a Novel Dendrimer-Based Demulsifier and Its Application in the Treatment of Typical Diesel-in-Water Emulsions with Ultrafine Oil Droplets. *Energy Fuel* **2014**, *28*, 5998–6005. [CrossRef]

27. Xinliang, Y.; Chi, A. Demulsification Performance and Mechanism of Demulsification of a Dendritic Polyamidoamine. *Chem. Technol. Fuels Oil* **2016**, *52*, 306–309. [CrossRef]

28. Hao, L.; Jiang, B.; Zhang, L.; Yang, H.; Sun, Y.; Wang, B.; Yang, N. Efficient Demulsification of Diesel-in-Water Emulsions by Different Structural Dendrimer-Based Demulsifiers. *Ind. Eng. Chem. Res.* **2016**, *55*, 1748–1759. [CrossRef]

29. Bi, Y.; Li, W.; Liu, C.; Xu, Z.; Jia, X. Dendrimer-Based Demulsifiers for Polymer Flooding Oil-in-Water Emulsions. *Energy Fuel* **2017**, *31*, 5395–5401. [CrossRef]

30. Wang, J.; Li, C.Q.; Li, J.; Yang, J.Z. Demulsification of Crude Oil Emulsion Using polyamidoamine dendrimers. *Sep. Sci. Technol.* **2015**, *9*, 2111–2120. [CrossRef]

31. Zhang, L.; Ying, H.; Yan, S.; Zhan, N.; Guo, Y.; Fang, W. Hyperbranched poly(amido amine) as an effective demulsifier for oil-in-water emulsions of microdroplets. *Fuel* **2018**, *211*, 197–205. [CrossRef]

32. Zhang, L.; Ying, H.; Yan, S.; Zhan, N.; Guo, Y.; Fang, W. Hyperbranched poly(amido amine) demulsifiers with ethylenediamine/1,3-propanediamine as an initiator for oil-in-water emulsions with microdroplets. *Fuel* **2018**, *226*, 381–388. [CrossRef]

33. Helden, L.; Dietrich, K.; Bechinger, C. Interactions of colloidal particles and droplets with water-oil interfaces measured by total internal reflection microscopy. *Langmuir* **2016**, *32*, 13752–13758. [CrossRef] [PubMed]

34. Zhang, P.; Wang, H.; Liu, X.; Shi, X.; Zhang, J.; Yang, G.; Sun, K.; Wang, J. The dynamic interfacial adsorption and demulsification behaviors of novel amphiphilic dendrimers. *Colloids Surf. A* **2014**, *443*, 473–480. [CrossRef]

35. Liu, C.; Gao, C.; Yan, D. Synergistic Supramolecular Encapsulation of Amphiphilic Hyperbranched Polymer to Dyes. *Macromolecules* **2006**, *39*, 8102–8111. [CrossRef]

36. Yanez Arteta, M.; Campbell, R.A.; Nylander, T. Adsorption of Mixtures of Poly(amidoamine) Dendrimers and Sodium Dodecyl Sulfate at the Air-Water Interface. *Langmuir* **2014**, *30*, 5817–5828. [CrossRef]